SYNOPTIC SURVEY OF THE INTERACTION OF SEA AND ATMOSPHERE IN THE NORTH ATLANTIC

BY J. BJERKNES

FREMLAGT I VIDENSKAPS-AKADEMIETS MØTE DEN 9DE FEBRUAR 1962

Summary. The North Atlantic sea surface temperatures on record from the files of the U.S. Weather Bureau, and from the Danish Meteorological Office and the Conseil Permanent International pour l'Exploration de la Mer, Copenhagen, have been studied as to the *meteorological cause* for their year to year, and longer, fluctuations.

A long trend of cooling north of 50°N extending from the 1890's to the early 1920's, goes parallel to a strengthening of the Iceland low, and the subsequent warming until the early 1940's is associated with a weakening of the Iceland low. During the long trend of northern cooling, the water warmed up west and north of the intensifying subtropical high, presumably by increased wind and Gulf Stream advection. The northern cooling and the Gulf Stream warming intensified the baroclinicity along 50°N. By *oceanic feedback* also the atmosphere must have increased its baroclinicity along that latitude, thus intensifying statistically the energy of cyclogenesis along the atmospheric Polar Front. This, in turn, must have led to the progressively deeper Iceland low.

During the long cooling trend in the north from the 1890's to the early 1920's, up and down trends of two to five year duration were superimposed. Their maximum amplitudes in pressure gradient and sea temperatures were observed half way between Iceland and the Azores. In these trends the ocean always cools when the prevailing west wind strengthens and warms up during the phases of decreasing west wind.

Fragmentary evidence indicates that the Canary Current, the North Equatorial Current, and the Caribbean cool off when the trade-winds intensify and at that stage presumably absorb heat (sensible and latent) at an increasing rate. This oceanic thermal feedback can be expected to increase the general atmospheric circulation and prolong the one-way tend. An analogous trend of decreasing atmospheric circulation can be visualized to be similarly prolonged.

The mechanism of trend reversals is still rather obscure, but can possibly be better judged when it is found out whether they are localized to the North Atlantic or occur in the same phase also in the North Pacific.

Orientation for meteorological readers on some North Atlantic hydrographic features. Figure 1, published by A. DEFANT in 1941, and still valid in its major features, represents the available knowledge about the topography of the sea level of the North Atlantic Ocean. Hence it also represents an approximation to the

geostrophic streamlines immediately under a shallow wind drift layer. Only near the jet-like currents like the Gulf Stream near America or the coastal currents past southern Greenland, do the simple geostrophic rules require corrections for lateral eddy friction and convective accelerations.

The general shape of the geostrophic streamlines satisfies the principle enounced by SVERDRUP (1947) that in order to maintain at each locality a constant ocean level, poleward geostrophic flow, with its inherent horizontal convergence, must occur where the integrated transport of the drift current shows horizontal divergence, and equatorward flow with geostrophic divergence must occur under a drift current with mass transport convergence. Consequently, the proper place for poleward flow is under the cyclonic wind systems in the north where the "Ekman drift", 90° to the right of the wind direction, provides for surface divergence, and for equatorward flow under the anticyclonic wind system in lower latitudes, where the corresponding EKMAN drift is convergent.

This SVERDRUP principle, later amplified by MUNK (1950), STOMMEL (1957), and FOFONOFF (1960—61) is strictly valid only where the geostrophic current vanishes well above the bottom of the ocean. The bottom topography introduces additional constraints on the deep geostrophic currents all the way up to the surface, such as are seen in the sharp bends at the "Tail" of the Newfoundlands Banks, at Flemish Cap (47°N 45°W), and at the mid-Atlantic Ridge from Iceland to the Azores.

The Sverdrup principle explains satisfactorily the important branching process of the Gulf Stream beginning at the Tail of the Grand Banks. All of the branches flowing north of the Azores will be referred to collectively as the North Atlantic Current (ISELIN's (1936) terminology). The northernmost branch flows along the oceanic Polar Front, which can be followed from the Tail of the Grand Banks in a general northeastward and then eastward direction to the Mid-Atlantic Ridge at 51°N. Its continuation northward toward Iceland is less sharply defined, but in principle it would follow along the left flank of the farthest left branch of the North Atlantic Current, known under the name of the Irminger Current.

On approaching east Greenland the Irminger Current reaches the oceanic Arctic Front beyond which the East Greenland Current flows southwestward to Cape Farewell. The Irminger Current divides into one branch leading to the north coast of Iceland and another paralleling the East Greenland Current to Cape Farewell. The Arctic water of the East Greenland Current, although much colder than the Atlantic water of the Irminger Current, is less dense due to its low salinity and is confined to the Greenland shelf. West of Cape Farewell both Arctic and Atlantic water are represented in the northwestward flowing West Greenland Current. Most of the Atlantic water, while progressively sinking, branches to the left toward the Labrador coast where it turns south parallel to the Arctic outflow from Baffin Bay. The Arctic water is also here lighter than the adjacent Atlantic water and does not descend from the Labrador shelf. What is normally called the Labrador Current thus consists both of Arctic and Atlantic water. The Arctic core of the Labrador current can be followed past New-

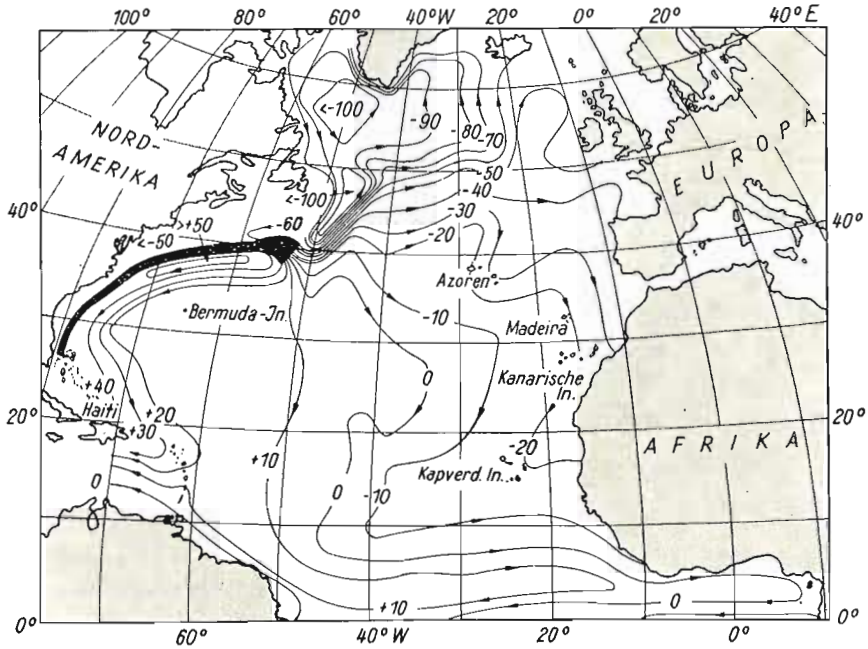

Fig. 1. Topography in dyn. cm of the surface of the North Atlantic Ocean. From A. Defant, 1941.

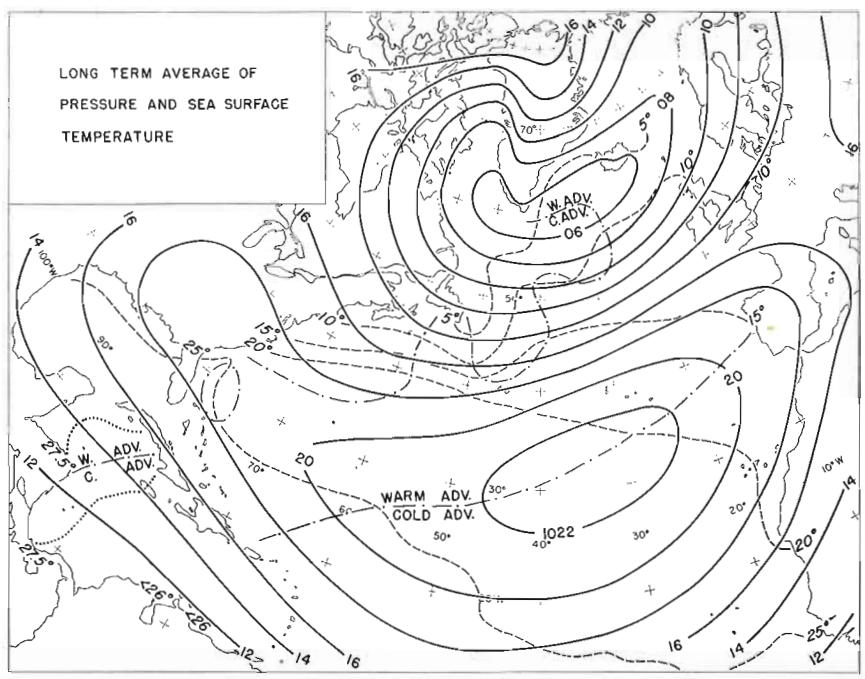

Fig. 2. Average annual isobars (solid), annual sea surface isotherms (dashed), and approximate prevailing limits (dotted) between warm and cold advection in the surface water.

foundland and along the eastern edge of the Grand Banks to the Tail at 43°N. At that place part of it submerges while the rest makes a sharp turn into northeastward direction parallel to the swift North Atlantic Current. Intensive meandering of the two currents on that stretch gradually raises the temperature and salinity of the water from the Labrador Current toward that of the adjacent Atlantic water.

The cyclonic current system described above receives from the outside the warm, salty, water masses of the Irminger Current and the cold, much less salty ones, from the East Greenland and the Labrador Currents. The excess of inflow at the surface must sink, as already described for part of the Irminger—Atlantic water, and feed a southward outflow of deepwater, estimated by SMITH, SOULE, and MOSBY (1937) to an annual average of 1.9 million m^3 per second. The same authors have, through their study of oceanographic profiles, been able to localize the most likely region for vertical convection from the winter-chilled surface water after elimination of the thermocline stability. It coincides with the trough of the ocean level off southwest Greenland on DEFANT's map in Fig. 1. According to the findings of the Meteor expedition in March, 1935, the ocean stratification permitted sinking to about 2,000 m depth also due south of Cape Farewell, between 57° and 55°N, and possibly continuing along the trough in the ocean level parallel to the southeast coast of Greenland.

The downwelling area coincides in location and shape with the average Iceland cyclone and its trough extension to the northern Labrador Sea (Fig. 2), in other words, it coincides with a region of EKMAN divergence of the surface water. That systematic wind effect tends to keep the thermocline shallow at the center of the oceanic vortex and it tends to maintain the observed dome shape of the deep water isopycnals at the core of the vortex.

Atmospheric variability from day to day and month to month will interfere with the smooth performance of the dynamic linkage outlined above. In particular, it is likely that an atmospherically dictated temporary change from EKMAN divergence to Ekman convergence is the trigger that releases the annual large scale convection in late winter, which, once started, may run by conversion of potential into kinetic energy within the deepwater.

The wind drift, which superposes itself on the geostrophic currents of Fig. 1, will also influence the sea surface temperature through warm or cold water advection. A brief survey of the wind drift mechanism is therefore in order at this stage. EKMAN's classical model of the drift current, reproduced in Fig. 3, contains all the necessary basic information: the pure wind drift at the surface of a homogeneous ocean deviates 45° to the right of the wind direction (assumed not to change with time) and turns with increasing depth more and more to the right (northern hemisphere) while decreasing in speed at such a rate that, in the hodograph shown at the base of the model, the arrow point of the wind vectors describes a logarithmic spiral with its center at the common vector origin. After having turned with depth to the direction opposite to the wind drift at the surface the drift vector has decreased to $e^{-\pi} = 1/23$ times its scalar value at the surface. For practical purposes the depth where the wind drift has turned around

180° has been defined as the depth of frictional influence. That depth is known to be of the order 50 m in the Iceland region and increases at given wind velocity as $1/\sqrt{\sin \varphi}$ toward the equator. The "friction layer" above that depth has in the northern hemisphere an integrated mass transport directed 90° to the right of the wind direction. This is the "EKMAN drift" already referred to:

$$T_y = -\frac{\tau_x}{\varrho\, 2\, \omega \sin \varphi}$$

where the x-direction runs along the wind direction, τ_x stands for the wind stress and ϱ for water density, while $2\ \omega \sin \varphi$ is the Coriolis factor.

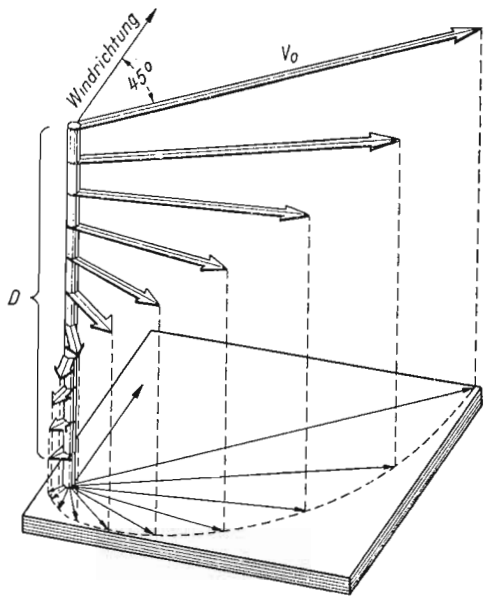

Fig. 3. Model of the pure wind drift current. From Ekman, 1905.

In our applications the atmospheric isobar is a more convenient coordinate axis than the wind direction. In the isobaric coordinate system the EKMAN drift has a slight component forward along the geostrophic wind in addition to the cross-isobaric component, which is still the stronger of the two. At the ocean surface, instead of the equality of drift current components along and across the wind direction, we get in the isobaric system a greater component along than across the isobar.

The empirical formula

$$v = \frac{0.0127\ W}{\sqrt{\sin \varphi}}$$

relates the surface speeds of the pure drift current v to the wind velocity W. As a rule of thumb, which is good enough in our estimates, the average water drift in middle latitudes is only 1.5 per cent of the vectorially averaged wind.

As can be seen from Fig. 2, the long time average of the drift current is very weak in the western Atlantic, due to the small vectorial resultant wind, while from Newfoundland to northwest Europe it must be stronger, with a maximum west of Ireland. At the same time the geostrophic part of the water motion (Fig. 1) is strong, up to 150 cm/sec, in the Gulf Stream off the American coast, tapering off to speeds comparable with the drift current near Europe and Iceland. Hence, the vector sum of the geostrophic and the drift current is dominated by the former in the western Atlantic, whereas eastward from Newfoundland the meteorologically dominated drift current must become an increasingly important part of the total surface current.

Between Newfoundland, Iceland, and the British Isles the geostrophic component

of the surface current heads on the average a little farther northward than the average geostrophic motion in the atmosphere, while the pure drift components, in accordance with theory, deviates to the right of the atmospheric isobars (but less than 45°). Therefore we do not go far wrong by approximating the direction of the total surface current with that of the atmospheric isobars.

With the above general justification we have introduced in Fig. 2, in addition to the annual average sea isotherms, also the boundaries between warm and cold advection of surface water obtained under the approximate assumption of water motion parallel to the annual atmospheric isobars. With analogous justification the approximate picture of the time change of water advection at the ocean surface has been derived in Figs. 14 and 19 from the time change of the atmospheric circulation. It should, however, be clearly understood that the zero advection lines are merely entered as an orientation for locating the large-scale geographical changes in surface water advection, and are not an expression for precise physical theory.

One specific reason for minimizing the estimate of thermal advection in the ocean crosswise to the right of the geostrophic wind applies to the belt of westerlies. The cross-isobar component of the surface drift current goes there toward warmer and lighter water, and part of the surface water is apt to submerge wherever a baroclinic zone is encountered. With the North Atlantic Current splitting, as it does, into many branches, such bacolinic barriers would exist in great numbers and would count against the general cooling effect of the cross-isobaric advection.

In the end it is, of course, observations that must give the proper estimates of the water advection and we hope that the observations organized into the maps following later in this paper will give a little information in that respect.

In the *low latitude belt* in Fig. 1, the geostrophic flow in the ocean deviates systematically equatorward relative to the geostrophic flow in the atmosphere. The forces moving the water particles at the ocean surface are shown in their typical orientation in the vector diagram in Fig. 4. (From DEFANT, 1941). The pressure gradient force points "downhill" toward the southeast, the skin friction points southwestward parallel to the surface wind, and the Coriolis force, in order to establish balance, must point somewhere near northwards. The stronger the wind at a given ocean pressure gradient, the more the Coriolis force must point east of north to establish zero acceleration. Such a set of forces must operate in order to maintain the surface drift which in the North Equatorial Current is observed to point a little north of westward, while below the friction layer the geostrophic flow points definitely south of westward.

What is important for our problem is to know whether an increase of the trade-wind will cool or warm the ocean surface. The verdict of the observations, presented by BULLIG (1954) and long before him by LIEPE (1911), is definitely in the sense that an increasing trade-wind does cool the ocean. Recently performed spectral analysis of BULLIG's data by RODEN (1961) confirms this result.

Despite these concordant findings, the suspicion might still remain that LIEPE's and BULLIG's sea temperature data on the Europe to South America shipping lane

could be locally influenced by upwelling water from the African coast, and more so the stronger the northeast trade-wind. The statistics by NEUMANN and PANDOLFO (1958) for a test field between 16° and 20°N and 34° to 36°W, settles the question for the mid-ocean trade-wind region, because also there the sea temperature and the strength of the tradewind are negatively correlated.

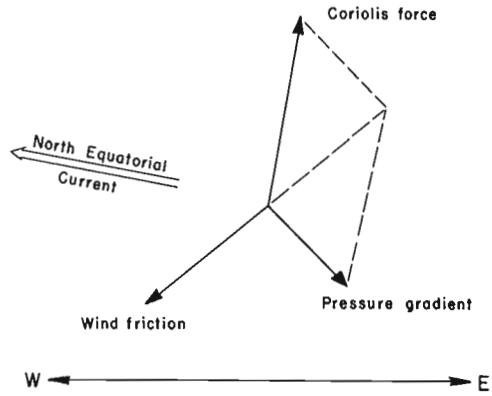

Fig. 4. Balance of forces for unaccelerated particles at the surface in the North Equatorial Current. From Defant 1961.

Three processes apparently join to firmly establish that relationship: the evaporation, the transfer of sensible heat, and the cold advection by the North Equatorial Current all tend to produce local cooling of the sea surface and more so the stronger the trade-wind. The opposite advective effect of the surface component of current away from the equator, shown in Fig. 4, is evidently overcompensated.

Reference will be made in the following text to SVERDRUP—JACOBS (1942) map of the annual radiative heat surplus of the North Atlantic Ocean, and those of the net heat transfer of that ocean to the atmosphere. The maps are easily available in several oceanographic text books and will not be reproduced here.

A. Time series of sea temperature in a profile Iceland-Azores. Figure 5 gives an orientation concerning the fluctuations of sea surface temperature in six selected ocean test fields centered around longitude 27.5°W and extending from western Iceland, 61.5°N to the Azores 37.5°N. The fluctiatuons in the strength of the middle latitude westerlies are represented on the same time scale by the annual mean sea level pressure at Vestmannaeyar (SW Iceland) and Ponta Delgada (Azores) and supplemented by the curve of Ponta Delgada minus Vestmannaeyar pressure. In order to facilitate the visual identification of the long trends a 19-year binomial smoothing of all curves has been entered in dotted lines.

If we define the long trends by the dotted lines, we see that the epochs of weak Iceland cyclone (maxima in the Iceland pressure curve) occurred in the middle 1850's, in the late 1870's and again in the late 1880's.

Thereafter came a long trend of intensification of the Iceland low leading to the lowest pressures of the whole record in the early 1920's. Then a relatively steep pressure rise set in leading to the weakness of the Iceland low in the early 1930's, and even more so in the early 1940's. The latter maximum in the Iceland pressure curve practically equalled that in the late 1880's, but was a little less pronounced than the maximum in the late 1870's and the middle 1850's.

The sea temperature record in the ocean fields centered 61.5° and 57.5°N started

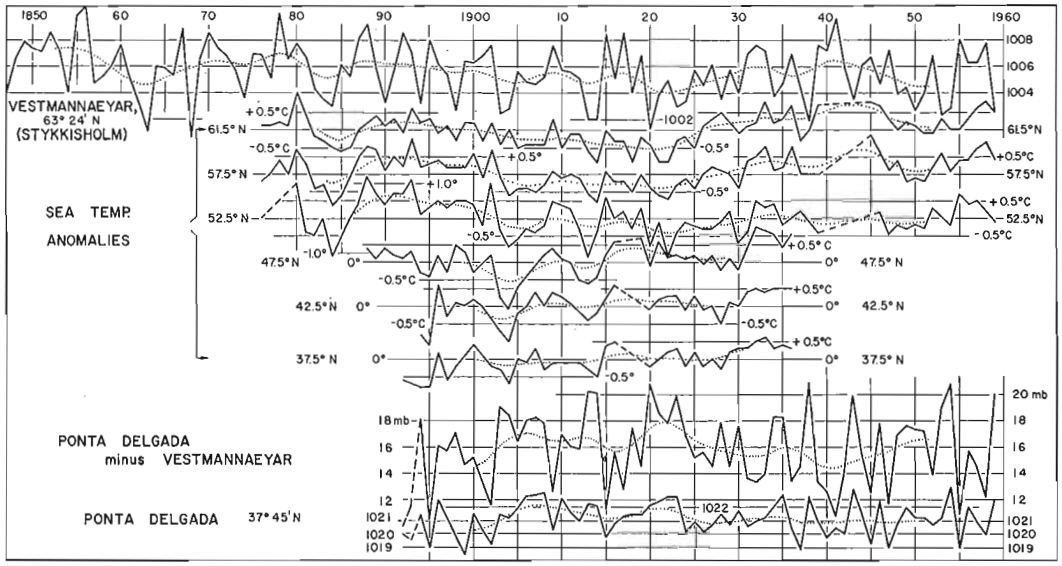

Fig. 5. Time series of annual sea temperatures in a profile Iceland-Azores. Top curve: Time series of annual sea level pressure for Vestmannaeyar (extrapolation before 1881 based on Stykkisholm). Bottom curves: Time series of annual Ponta Delgada minus Vestmannaeyar sea level pressure (zonal index), and time series of annual sea level pressure for Ponta Delgada.

in 1876 and that of the next field to the south (52.2°N) became continuous four years later. The smoothed curves for those three fields show a fair resemblance to the smoothed Iceland pressure curve in all major features. In particular, the long falling trend before 1922 and the subsequent rise[1] are unmistakeably parallel features in sea temperature and Iceland pressure.

The correlation coefficients between the smoothed Iceland pressure curve and each of the correspondingly smoothed sea temperature curves are:

Table 1. *Sea Temperature versus Vestmannaeyar pressure, both identically smoothed.*

Period	Test field	Coefficient
1882—1939	61.5°N	0.66
1882—1939	57.5°N	0.79
1882—1939	52.5°N	0.80
1894—1928	47.5°N	0.18

The closest correlation, about +0.8, is found between the Iceland pressure and the sea temperature in the belt of westerlies between 60° and 50°N. South of 50°N

[1] For further statistical evidence of these long trends in sea temperature see also NEUMANN and PANDOLFO (1958).

the sea temperature correlates only slightly with the Iceland pressure. All the correlation coefficients are positive, hence indicating a warmer ocean surface when the Iceland cyclone has less than normal depth.

The conditions at the center of the Iceland low are represented by the field marked 61.5°N. There the correlation between pressure and sea temperature is a little less firm than in the adjacent belt of prevailing cold advection westerlies.

The identification of a possible lag between the intensity changes of the Iceland low and the resulting change of the sea temperature would be of considerable interest. At this stage we will only point out as an example that the sea temperature minimum at 61.5°N in 1885 and the maxima in 1889 and 1893 lag one year behind the corresponding extremes in the Iceland pressure curve, whereas the sea temperatures in the two adjacent fields to the south show no lag.

The test of long trend relationships between Ponta Delgada pressure and the sea temperature in the adjacent fields to the north (all identically smoothed) gives the following result:

Table 2. *Sea temperature versus Ponta Delgada pressure, both identically smoothed.*

Period	Test field	Corrrelation Coefficient
1900—1928	52.5°N	—0.45
—	47.5°N	0.08
—	42.5°N	0.11
—	37.5°N	—0.22

The correlations are small and of varying sign, quite different from what was found in Table 1.

The correlations of the smoothed sea surface temperature anomalies near the line Vestmannaeyar—Ponta Delgada with the smoothed pressure differences between these two points are given in Table 3 (on the following page).

Table 3. *Sea temperature versus pressure difference Ponta Delgada minus Vestmannaeyar. All data identically smoothed.*

Period	Test field	Correlation coefficient
1900—1928	61.5°N	—0.34
—	57.5°N	—0.82
—	52.5°N	—0.82
—	47.5°N	0.18
—	42.5°N	0.33
—	37.5°N	—0.37

The high negative correlations at 57.5° and 52.5°N express the same dependence of sea temperature on the strength of the westerlies as do the high positive correlations for those same fields in Table 1, because the variations with time of the Azores minus Iceland pressure difference are mainly decided by the great variability of the Iceland pressure.

The northernmost field (61.5°N) shows, as could be expected, definitely less dependence of sea temperature on the strength of the westerlies than do the neighboring fields to the south. It is also worthy of note that the sea temperature of the northernmost field does depend on the depth of the Iceland cyclone, as shown in Table 1, whereas it depends much less on the Azores to Iceland pressure gradient.

The fields south of 50°N, according to Table 3, do not follow the rule established north of that latitude. The fields 47.5°N and 42.5°N even show a faint tendency for warmer water when the westerlies, as defined by the Azores to Iceland pressure gradient, are stronger than normal.

So far, all the correlations discussed have been obtained from the binomially smoothed (dotted) curves in Fig. 5. As a final test of ocean-atmosphere correlations in the Iceland-Azores profile we now eliminate the long trends and correlate the shorter period residuals of sea temperature to the corresponding residuals in the Azores minus Iceland pressure change. The result is shown in Table 4.

Table 4. *Short period residuals of sea temperature versus short period residuals of pressure difference Ponta Delgada minus Vestmannaeyar.*

Period	Test field	Correlation Coefficient
1900–1928	61.5°N	−0.48
—	57.5°N	−0.64
—	52.5°N	−0.72
—	47.5°N	−0.65
—	42.5°N	−0.45
—	37.5°N	−0.45

All fields now show the tendency for negative sea temperature anomaly during years of positive anomaly of the westerly winds, and most strongly so in the field centered at 52.5°N.

Tables 3 and 4, considered jointly, present us with the question: why is the sea temperature between 50° and 40°N correlated positively with the long trend variations and negatively with the short term variations of the westerlies? We will return to that question in Section B 2.

Our next problem is to determine the main physical processes in ocean and atmosphere whose operation through the years leads to the statistical relationships contained in Tables 1 to 4. In the choice of method for this search the present author has been guided by his study of the monumental investigation by HELLAND-HANSEN and NANSEN

(1917). These great pioneers gained their results concerning the causes of fluctuations in sea temperature from a thorough analysis of time series similar to those in Fig. 5, painstakingly compiled for the years 1898 to 1910 mainly from the shipping lane New York — British Channel.

Their conclusion was that very little evidence could be found of positive and negative sea temperature anomalies being transported along the Gulf Stream System at the speed of the the water motion. Much greater temperature anomalies of the ocean surface were found to be produced by wind anomalies and to appear, and later disappear, over large sections of the North Atlantic almost simultaneously. The wind anomalies were represented in the statistical treatment by the monthly component of geostrophic wind transverse to the direction of the long term average geostrophic wind for the same month. This method thus mainly correlates the sea temperature changes to the anomalous occurrence of north and south components of wind in the belt of average westerlies, whereby the cooling of the ocean by northerly and warming by southerly wind components clearly shows up.

The present much smaller investigation will be based on synoptic maps of a) the sea temperature anomalies in selected years, or groups of years, representing extreme conditions, and b) the corresponding synoptic pressure fields in the atmosphere. Maps of changes of sea temperature, during selected one-way "trends" in that element, will also be used, together with the isallobaric maps describing the change in atmospheric circulation from beginning to end of the trend under consideration.

Despite the difference in tools, I feel that the present investigation is a direct follow-up of that of HELLAND-HANSEN and NANSEN forty-four years ago. Its justification lies not in any revolutionizing of their ideas on ocean-atmosphere interaction, but in the utilizing of longer records of basic data.

B. Synoptic presentations of the trends in sea temperature.

1. *The short trends of 2 to 5 years.* It can be expected that the simplest synoptic patterns of sea temperature change will result in the case of trends which are almost in phase all the way from Iceland to the Azores such as shown in Table 4. Moreover, the amplitudes involved in these short trends of 2 to 5 years are so great that their cause should not be too difficult to find. We have selected from the chronology diagram, Fig. 5, the years 1902, 1909, and 1915 to represent the warm, and 1904, 1913, and 1920 to represent the cold extremes in the short-period system. The successive cooling and warming trends are represented synoptically in Figs. 6 to 10 by dashed isollotherms of annual sea temperature. On the same maps the isallobars of annual pressure are shown in fully drawn lines. Reference to the long-term average annual fields of pressure and sea temperature can be obtained in Fig. 2.

The maps in Figs. 6 to 10 are strikingly similar in their major features. The isallobars show the extreme pressure changes in the Iceland-Southern Greenland area, and in each case there is a center of opposite pressure change west of the Azores. An

extreme change of sea temperature is always found between the two poles of opposite pressure change, the average location of the isallotherm extreme being near 35°W and a little north of 50°N. The sign of the sea temperature change is always negative while the Iceland low intensifies, and positive while the Iceland low weakens.

Figure 11 illustrates the average conditions for the three years of weak westerlies (low index) and Fig. 12 the three years of much stronger westerlies (high index). The dashed lines, indicating the field of sea temperature anomaly, again show the positive anomaly in the belt of westerlies to occur in low index years and the negative anomalies in high index years.

The differences in pressure and sea temperature between the average high index year and the average low index year is shown in Fig. 13. The isallobars define a belt of rise extending from the United States to southern Europe, with a maximum exceeding 3 mb west of the Azores. The simultaneous pressure fall covers the Atlantic north of 50°N and exceeds — 6 mb in the Iceland to southern Greenland area. The maximum drop in sea temperature exceeds —1.5°C and is located a little north of 50°N, near the latitude of strongest isallobaric gradient. The average extent of the area of cooling (respectively warming from high index to low index years) is defined by two nodal lines, the eastern one running from Iceland by way of Ireland to northwestern Spain and the western one running from Newfoundland southeastward, keeping west of the Azores. These nodal lines can be identified in almost fixed positions also on the individual difference maps in Figs. 6 to 10.

Altogether the maps in Figs. 6 to 13 corroborate HELLAND-HANSEN's and NANSEN's findings from before 1910 and add the information that the ocean-atmosphere system shows a distinctive tendency to repeat its geographic pattern of change although varying the rate of change from the one trend to the other.

The maximum range in sea temperature, 1.7°C, between low and high index years is almost one third of the normal seasonal range at the same location. Hence, there must be considerable unbalance in the heat budget of the sea surface layer during the up- and down-trends in the short period system, especially so during the two-year fall 1902—04 and two-year rise 1913—15.

In seeking the physical processes most likely to be responsible for the unbalance of the heat budget we will apply the equation

$$\varrho\, c \int_0^{\text{year}} \frac{\partial T_w}{\partial t}\, dt = \int_0^{\text{year}} Q_r dt - \int_0^{\text{year}} Q_a dt + \int_0^{\text{year}} Q_v dt,$$

which expresses the fact that the year to year change of sea surface temperature T_w of a fixed unit volume (cm^3) results from: the integrated radiation surplus, Q_r, of the surface water, minus the integrated heat supply, Q_a, (latent and sensible) from ocean to atmosphere, plus the integrated effect of heat advection, Q_v, that is, the convergence of heat flux by ocean currents. If we think of the "surface water" as comprising the whole thickness z_o of the water layer with an appreciable annual temperature change,

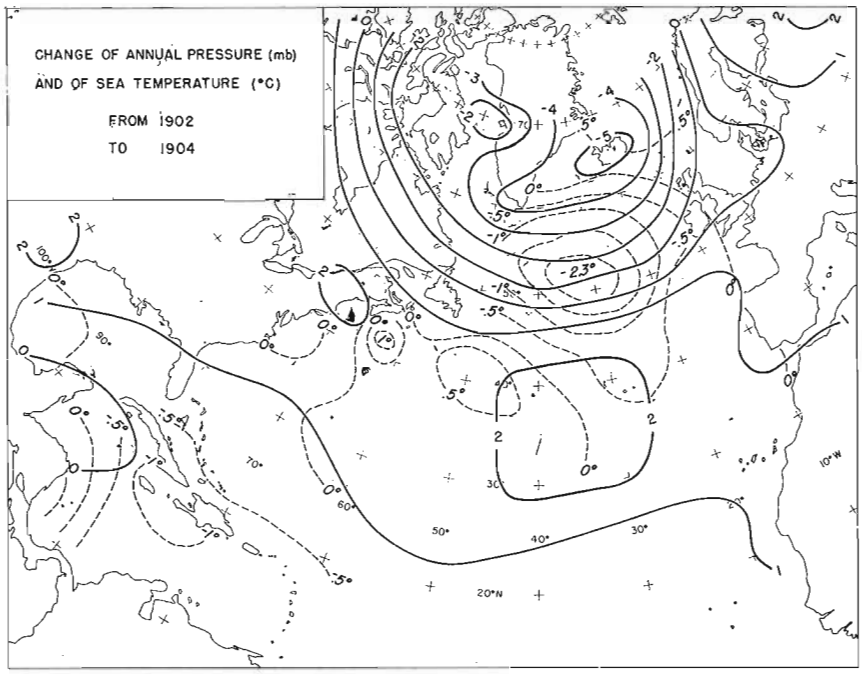

Fig. 6. Change of annual pressure and of sea temperature from 1902 to 1904.

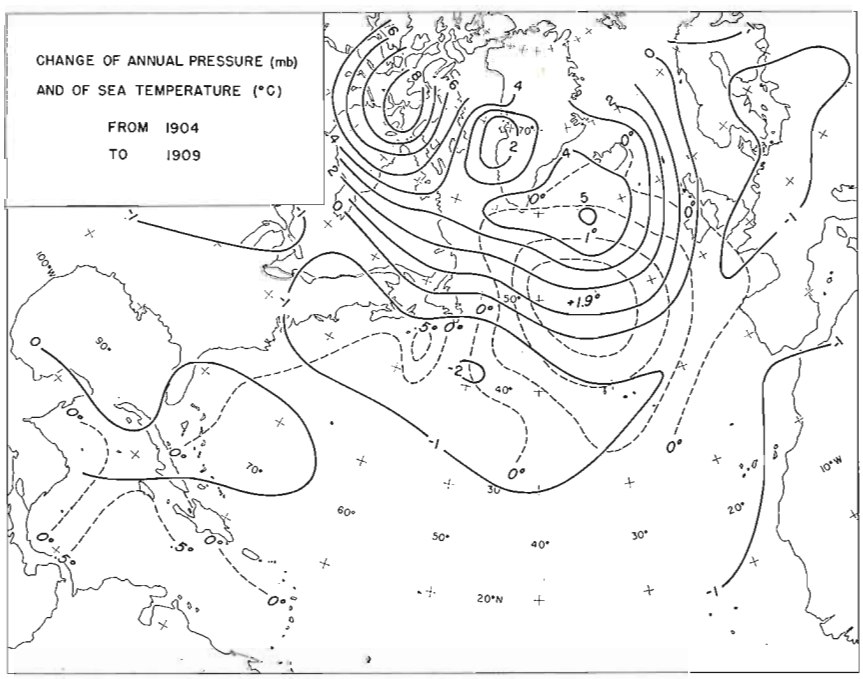

Fig. 7. Change of annual pressure and of sea temperature from 1904 to 1909.

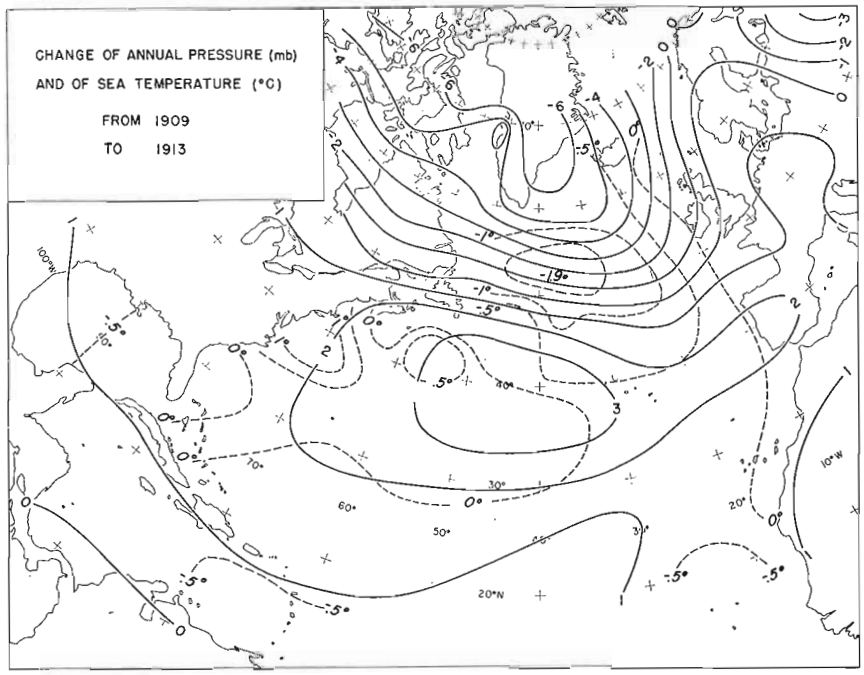

Fig. 8. Change of annual pressure and of sea temperature from 1909 to 1913.

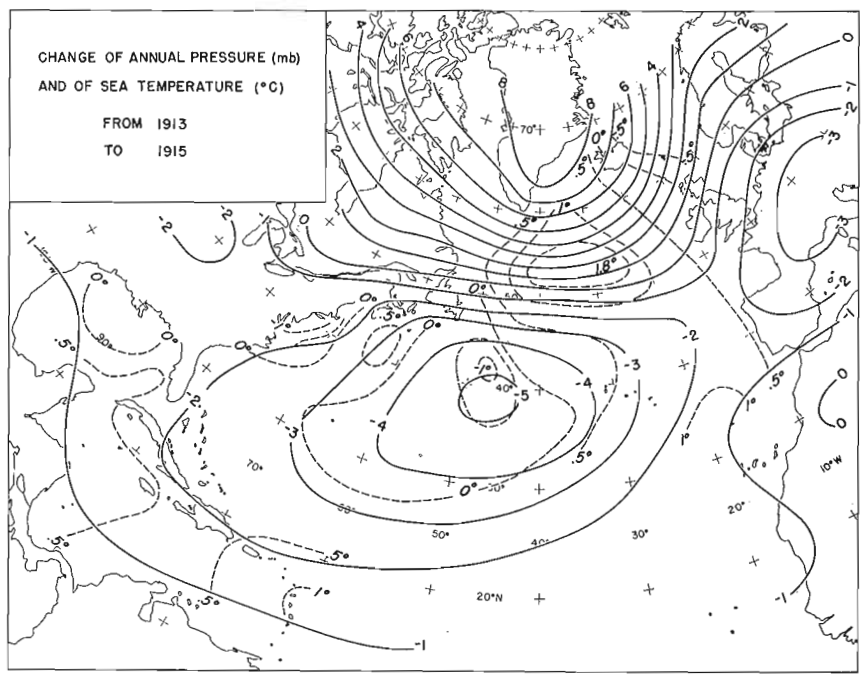

Fig. 9. Change of annual pressure and of sea temperature from 1913 to 1915.

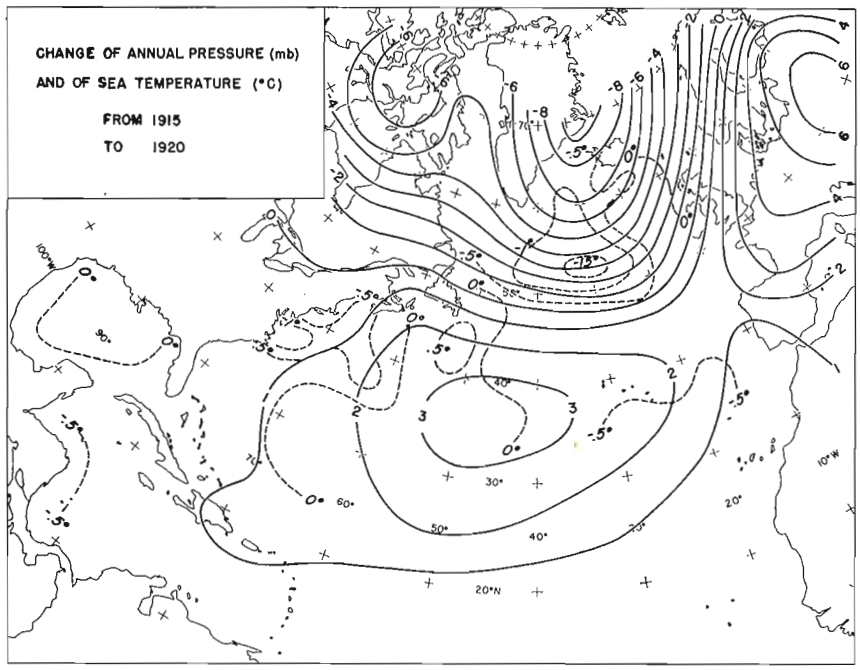

Fig. 10. Change of annual pressure and of sea temperature from 1915 to 1920.

the heat budget is also influenced by the large and small scale vertical flux of heat Q_{z_0} through the surface $z = z_o$. In that case the $\frac{\partial T_w}{\partial t}$ term must be depth averaged and multiplied by the number z_o of unit volumes in the column:

$$\varrho\, c \int_0^{\text{year}} \int_0^{z_0} \frac{\partial T_w}{\partial t}\, dt\, dz = \int_0^{\text{year}} Q_r dt - \int_0^{\text{year}} Q_a dt + \int_0^{\text{year}} \int_0^{z_0} Q_v dt\, dz + \int_0^{\text{year}} Q_{z_0} dt\,.$$

Most of the year to year change in stored heat would be recorded by integrating the left hand term down to the depth of 300 m, where the seasonal heat impulse from above has decreased to a small fraction of its value at the surface (PATULLO 1957).

In the deep narrow geostrophic currents temperature change from year to year by varying advection may be significant perhaps down to 1000 m, but most of the variability in Q_v must lie near the surface, probably within the realm of the drift current.

Consulting now the SVERDRUP-JACOBS maps concerning the normal annual heat balance at fixed location within the region of maximum rate of change of temperature in the 2 to 5 year trends, we find, for a point at 50°N 35°W, within the northernmost branch of the North Atlantic Current, that the heat loss Q_a to the atmosphere is offset by about equal amounts of heat supply from net radiation Q_r and warm water advec-

tion Q_v. Our problem is next from the map evidence in Fig. 13 to find the physical rea-reason for the unbalanced condition of the surface water heat budget.

The mere fact that maximum cooling or warming rates in the 2 to 5 year trends coincide geographically with the belt of greatest increase, respectively decrease, of the prevailing westerlies points to

$$Q_a = kW\left[(e_w - e) + 0.64\,(T_w - T_a)\,\frac{p}{1000}\right]$$

as the unbalancing factor. The loss of heat to the atmosphere is proportional to the average scalar wind W, and to the following bracket quantity which is bigger the colder is the air relative to the underlying water. The stronger the wind blows from the prevailing westerly direction, the colder will be the air it brings along from the cold western part of the ocean and, in winter, also from the cold continent beyond. It also adds to the importance of Q_a that the average wind direction in the region under consideration comes a little more from the north in high index than in low index years, as can be deduced from Fig. 13.

The influence of the wind components transversal to the prevailing wind can not be checked by Fig. 13. We do know that during the spells of northerlies the ocean would transfer more heat to the atmosphere than it receives during the reign of southerlies (see Petterssen 1961). But even if that surplus of cooling may be greater during low index than during high index years, we see from our Figs. 6 to 13 that invariably the high index years are the colder ones, which must be due to the strong westerlies.

None of the other budget items Q_r or Q_v, each of them normally only half as big as Q_a, could have produced the geographical pattern of anomaly of sea temperature in Fig. 13; but it is natural in Q_r and Q_v to seek the compensating action that eventually reverses the trend started by, say, an increase in Q_a. Let us first consider Q_r.

The radiation surplus Q_r of the surface water

$$Q_r = Q_i - Q_b$$

is the difference between the effective incoming short wave radiation, Q_i, and the effective back radiation in long wave, Q_b. SVERDRUP (1942) writes in his discussion of the heat budget of the oceans: "The diurnal and annual variations of the sea-surface temperatures and of the relative humidity of the air over the oceans are small, and the effective back radiation at a clear sky is therefore nearly independent of the time of day and of the season of the year, in contrast to the incoming short-wave radiation from the sun and the sky, which is subjected to very large diurnal and seasonal variations."

We can add for the purpose of our discussion that also from year to year the effective back radiation from the ocean must be unable to compensate for a major unbalance created by Q_a. In fact, although a colder ocean radiates less, the atmosphere, which has also become colder, reduces its radiation to the ocean even more with the result

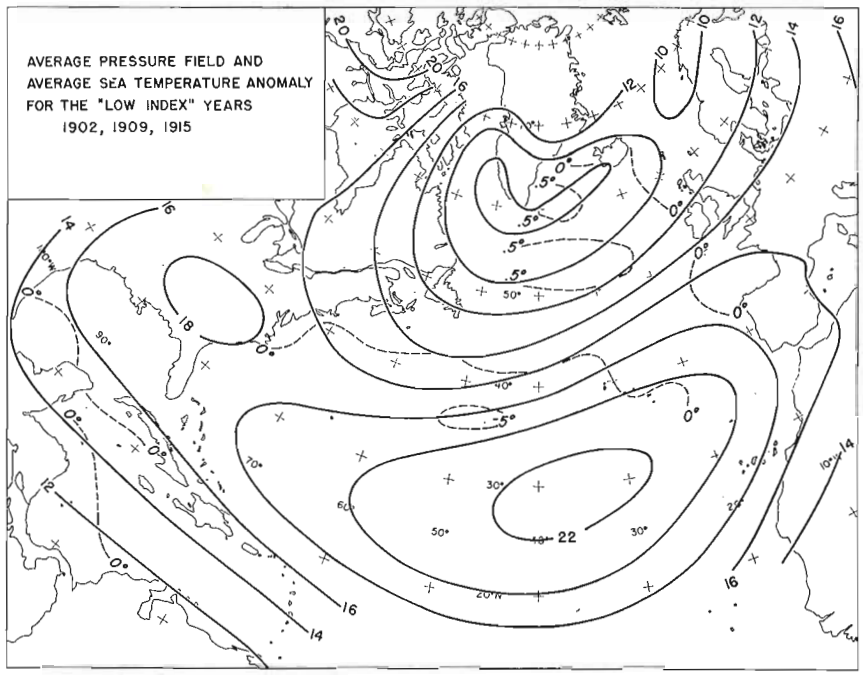

Fig. 11. Average pressure field and average sea temperature anomaly for the «low index» years 1902, 1909, 1915.

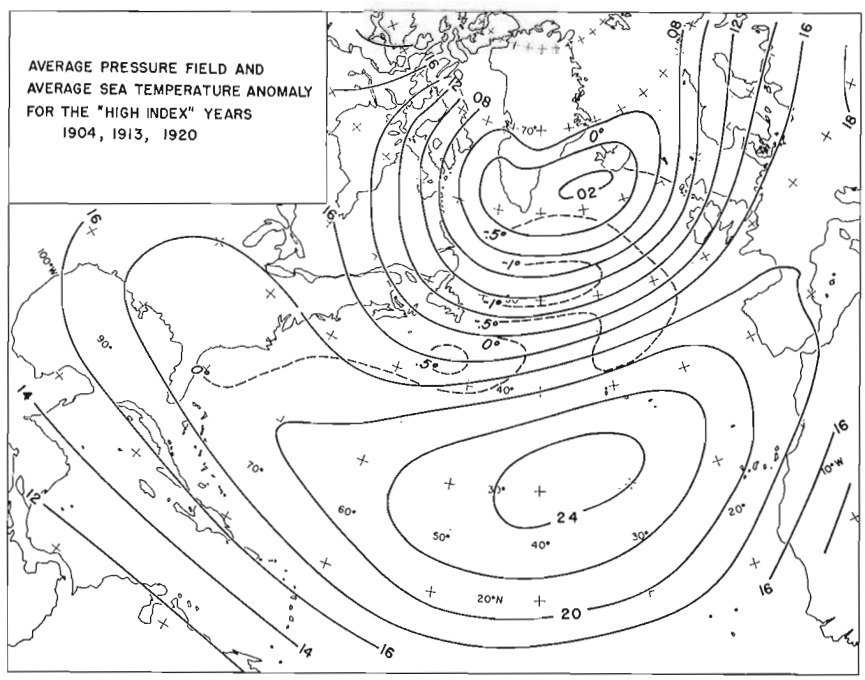

Fig. 12. Average pressure field and average sea temperature anomaly for the «high index» years 1904, 1913, 1920.

that under a clear sky the effective back radiation of the ocean, Q_b, *increases* with *decreasing* surface temperature (ÅNGSTRÖM 1920, SVERDRUP 1942).

Cloudiness influences both the effective incoming radiation to the ocean surface and the effective back-radiation from it. For the latter Sverdrup recommends the empirical formula

$$Q_b = Q_o\ (1-0.083\ C),$$

where Q_o is the back radiation at a clear sky and C is the cloudiness on the scale 1 to 10. For the effective incoming short-wave radiation a similar empirical formula by Mosby can be used.

$$Q_i = k\bar{h}\ (1-0.071\ C).$$

In it $\bar{h}$ is the average altitude of the sun, and the factor k depends upon the transparency of the atmosphere. According to the two empirical formulas above, the influence of cloudiness is percentually a little greater on Q_b than on Q_i, but since Q_i is systematically greater than Q_b (except in the arctic winter), the influence of increasing cloudiness is to reduce the raidiative surplus Q_r of the ocean. If a meteorological trend from low to high index does increase the cloudiness in the North Atlantic cyclone belt, which *a priori* may seem likely because evaporation increases, there is consequently no restoration of heat balance of the ocean water to be expected from the radiation processes. The analogous conclusion would of course be reached for the period of a cooling trend of the ocean.

A more complete discussion of the radiation balance of the ocean based on more modern research references can be found in J. MALKUS (1960). The final conclusion remains unchanged.

In the following discussion we will therefore assume that it is the interplay between the time changes of Q_a, the net transfer of heat to the atmosphere, and those of Q_v and Q_{z_0}, the advective heat supply and the up- or down-welling, which mainly decides the alternating trends of sea surface temperature.

Fig. 14, in conjunction with Fig. 2, will permit us to assess the sign of the changes in both Q_a and Q_v during the transition from low to high index circulation. Starting at the American coast, north of Cape Hatteras, we see from Fig. 2 that cold advection prevails in the atmosphere out to the Gulf Stream and a little beyond, and that the corresponding drift current also would tend to move the surface water between the coast and the Gulf Stream in the cold advection sense. Fig. 14 shows that there is relatively little change in that picture from low to high index years, but the slight isallobaric wind from the southwest must be interpreted as a somewhat decreasing frequency and severity of the cold waves from the continent. In response, as shown in Fig. 13, the ocean temperatures from the Carolina coast to southern Newfoundland rise a little. It must be admitted, however, that this warming of the ocean from low to high index did not occur in identical fashion on each of the maps in Figs. 6, 8, and 10, Much more analysis, in finer detail, will be needed for obtaining the full understanding of the ocean

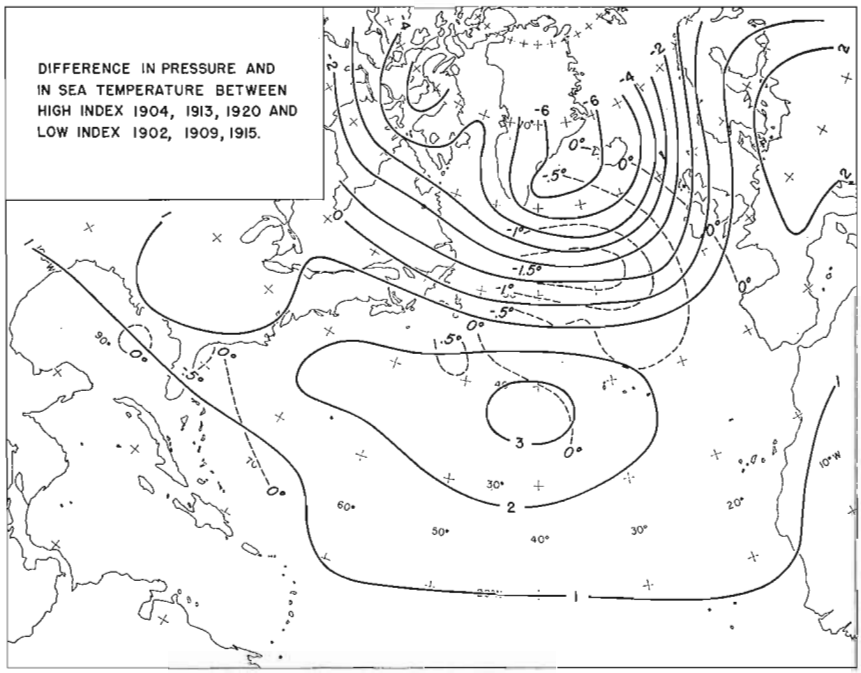

Fig. 13. Difference in pressure and in sea temperature between high index 1904, 1913, 1920 and low index 1902, 1909, 1915.

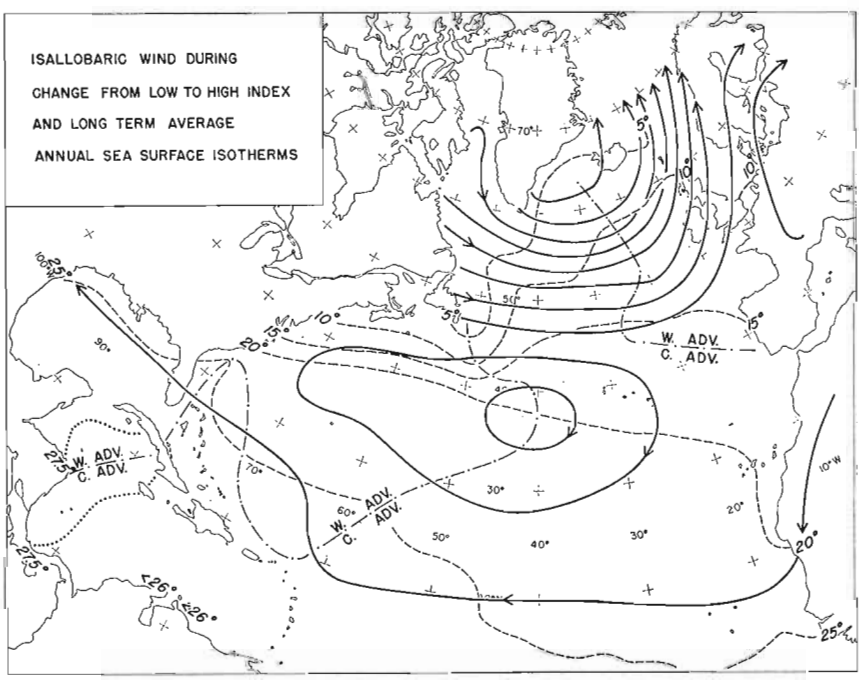

Fig. 14. The geostrophic isallobaric wind of the average trend from low to high index years. Dashed lines are the annual average sea isotherms, while dotted lines indicate borderlines between increasing cold advection and increasing warm advection.

response to atmospheric anomalies over the western Atlantic. Moreover, the years here selected to illustrate index changes of sea temperature in the central Atlantic are not the best to bring out typical patterns of change in the western part of the ocean.

The cold atmospheric advection, that, according to Fig. 2, is normal for the Labrador Sea and adjacent parts of the North Atlantic Current, becomes much stronger and more extensive from low to high index years. The isallobaric wind in Fig. 14 crosses sea isotherms from cold to warm in an area extending from Labrador—Greenland past the Azores into the trade-wind belt. As we have seen this agrees well with the extent and intensity of ocean cooling in Fig. 13, and with each of the low to high index cases of cooling in Figs. 6, 8, and 10.

In northwest European waters Fig. 14 indicates strongly increasing southwesterly winds from low to high index years, hence also a warm advection drift current adding vectorially to the normal warm water advection shown in Fig. 2. The sea temperature, however, only rises east of the nodal line Iceland—Ireland—NW Spain shown in Fig. 13. For the area west of that line we may have the following two effects jointly explaining the decreasing ocean temperature:

1) The transfer Q_a of heat to the atmosphere, although not indicated to be important on the base of the average map, Fig. 2, certainly is boosted by an "eddy term" contribution, the eddies being the individual storm centers. The rear of each cyclone contributes strongly to Q_a, while the front side has close to zero contribution because sea and air temperatures there differ so little. (see PETTERSSEN 1961).

2) The strongly increasing cyclonic vorticity of wind stress from low to high index over the ocean west of the British Isles may exert a noticeable upwelling effect, hence cooling the sea surface.

The center of greatest index cycle variability of sea surface temperature, around 53°N 35°W in Fig. 13, is located over the southern part of the Labrador-Irminger Sea, but big temperature amplitudes are found also over the adjacent branch of the North Atlantic Current. The nature of the sea temperature fluctuations in the northernmost branch of the North Atlantic Current is tentatively summarized in Fig. 15. The upper half of the diagram represents the observed negative correlation between sea temperature anomalies and the strength of the westerly winds. The time scale is not specified but can be assumed to be such that alternate one-way trends of 2 to 5 years are depicted with the seasonal periodicity removed by smoothing. The lower half of Fig. 15 shows, first, the anomaly of oceanic heat loss (sensible and latent) to the atmosphere. That negative quantity has presumably its maximum negative anomaly simultaneously with the maximum of the westerly winds. Secondly, the lower part of the diagram contains the hypothetical curve of the changing advective heat supply by the geostrophically controlled warm ocean current. This positive quantity in the local oceanic heat budget must be assumed to respond to a quickening atmospheric circulation around the Iceland low and have its maximum with some lag behind the maximum of the westerlies. At about half that lag time the anomalies of heat loss to the atmosphere and heat supply by water advection will be equal and opposite, so

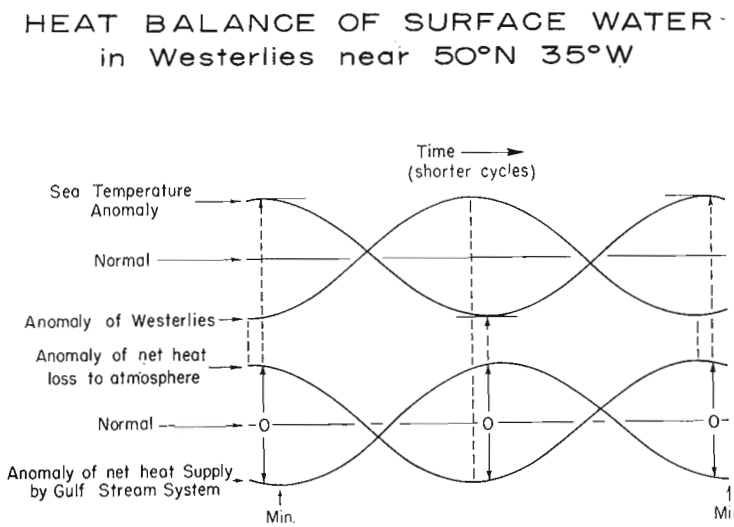

Fig. 15. Oscillations about the normal annual heat balance of the surface water in the northernmost branch of the North Atlantic Current at 35°W.

that the time derivative of the sea temperature becomes zero. The maxima and minima of sea temperature should therefore follow the minima and maxima of the westerlies with the very short lag shown in the upper part of Fig. 15, a lag which by-and-large remains concealed in the time series of annual values in Fig. 5.

The surface waters of the southern parts of the Labrador and Irminger Seas, which share with the adjacent North Atlantic Current the great variability of temperature in 2 to 5 year trends, must also have a heat budget dominated by the anomalies of heat loss to the atmosphere and compensating anomalies of heat gain by oceanic advection, with the anomalies of the radiative heat exchange playing a minor part. No quantitative estimates of the annual heat balance in the Labrador and Irminger Seas are available in the SVERDRUP-JACOBS maps (because of lack of all-year shipping), but we may assume that the following qualitative differences from the conditions in Fig. 15 would exist.

The annual heat loss to the atmosphere, Q_a, must be less north of than south of the oceanic polar front, in analogy with the conditions found by SVERDRUP and JACOBS in the "slope water" and the adjacent part of the Gulf Stream near North America. But, just as in the slope water, so also in the southern Labrador Sea the annual temperature anomalies at the surface become big due to the shallowness of the thermocline which limits the thermal impact of atmospheric anomalies to a thin oceanic surface layer. The annual sea temperature anomalies may also tend to become big because of the slow response of the oceanic heat advection to the southern Labrador and Irminger Seas. The heat supply must come, either by the roundabout Irminger Current continuing into the West Greenland Current and the eastern flank of the Labrador Current,

or by lateral mixing across the section of the oceanic polar front extending from the Tail of the Newfoundland Banks to the Mid-Atlantic Ridge. Quantitative data on these heat budget items are of course not available.

In the Labrador-Irminger Sea north of 55°N, where the heat loss to the atmosphere makes the thermocline vanish over great parts of the ocean by late winter, the sea surface temperature reaches an absolute minimum of about 3°C. Any further heat loss at the surface would be quickly redistributed over a depth of 2000 m and cannot very much depress the surface temperature. In that kind of hydrographic regime the late winter minimum temperature would be almost independent of the degree of atmospheric storminess; but the length of time during which the minimum temperature is established would presumably increase under the influence of high index stormy westerlies, and likewise the size of the area where deepwater and atmosphere are in contact. Summer temperatures of the ocean surface would obviously be lower than normal under high index conditions, since a very thin warm surface layer must bear the full impact of the heat loss to the atmosphere. This is clearly shown in maps (not published) which compare high index summers with low index summers.

The oceanic advection of heat reaches the northern part of the Irminger-Labrador Sea before it reaches the southern part, and the response to the Q_a-anomalies may be correspondingly faster.

Summing up, the Irminger—Labrador Sea would have its temperature changes controlled according to the same scheme of processes illustrated in Fig. 15 for the adjacent parts of the North Atlantic Current, but probably with more delayed response of oceanic heat advection to the primary meteorological anomaly of circulation.

2. *The long trends.* A map representative of the weak Iceland cyclone in the 1890's is shown in Fig. 16. It has been constructed by binomial smoothing of gridpoint values of pressure over the five-year period 1894—98. (The particular 5-year period was selected as the earliest one for which the sea temperature record south of 45°N and the pressure record at Ponta Delgada became complete.) In Fig. 17 another map, representative of the strong Iceland cyclone in the early 1920's, has been constructed by identically the same method for the five-year period 1920—24. The difference between the two maps is shown by isallobars in Fig. 18 together with the corresponding trend values of sea surface temperatures from 1894—98 to 1920—24.

The pressure change map, Fig. 18, shows a zero line crossing the Atlantic from Newfoundland to the Bay of Biscay. North of that nodal line there has been pressure fall, with greatest amounts in the Greenland—Iceland—Northern Scandinavian latitudes. South of the nodal line the Atlantic area has everywhere had pressure rise, with greatest amounts over a zone extending from Florida (near 27°N) to the Strait of Gibraltar (36°N). Briefly, this indicates a general strengthening of the Atlantic westerlies between 30°N and 65°N. The superimposed short-wave pattern in the northern part of that belt must have resulted from the great year to year pressure fluctuations which do not get sufficiently subdued by the five-year smoothing.

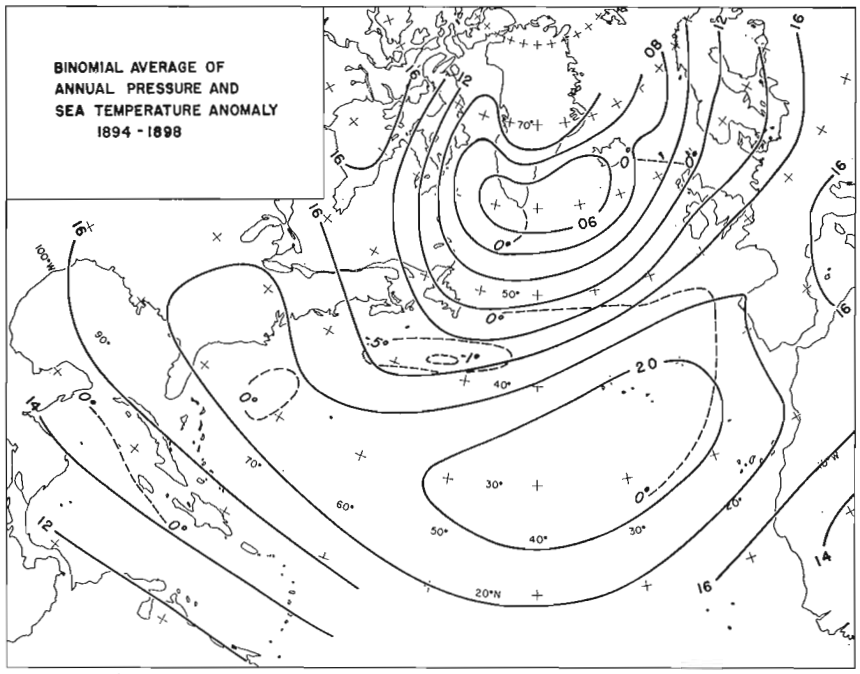

Fig. 16. Binomial average of the fields of pressure and sea temperature anomaly for low-index fiveyear period 1894—98.

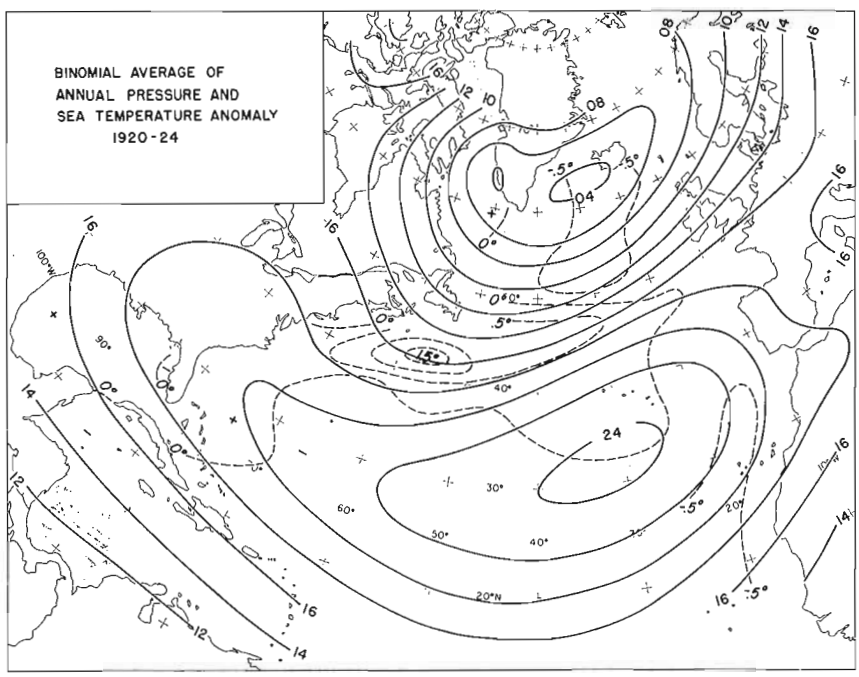

Fig. 17. Binomial average of the fields of pressure and sea temperature anomaly for high-index fiveyear period 1920—24.

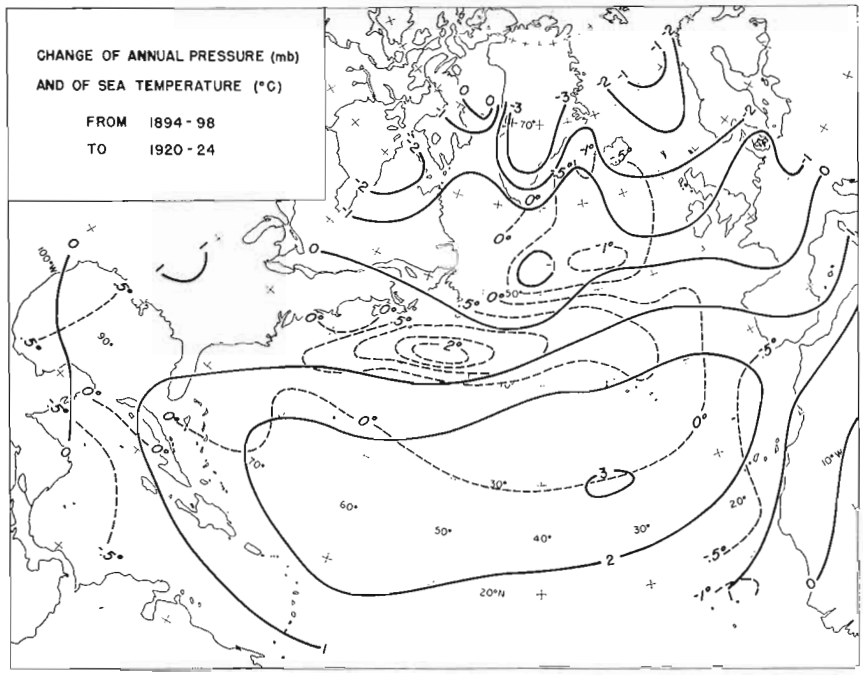

Fig. 18. Change of the fields of pressure and sea temperature from 1894—98 to 1920—24.

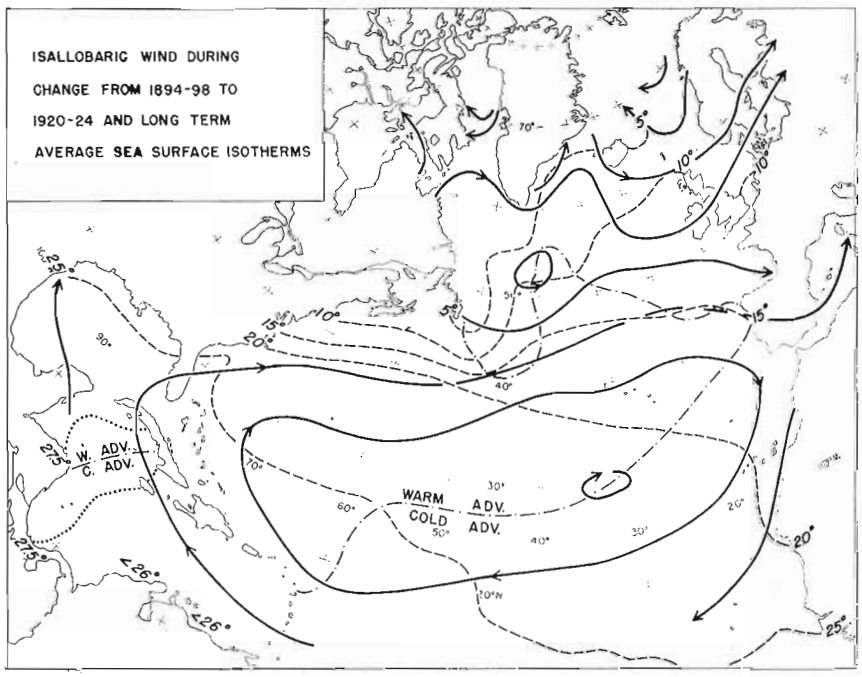

Fig. 19. The geostrophic isallobaric wind of the trend from low-index 1894—98 to high-index 1920—24 and the long term average isotherms of the ocean surface.

The isallobaric wind, corresponding to the pressure changes from the 1890's to the 1920's, is shown in Fig. 19 together with the annual sea surface isotherms. An increase of warm advection can be seen to have taken place from the Bahamas along the North American coast and thence across the ocean past the Azores. Correspondingly increased cold advection is seen to extend from southern Greenland—Iceland to the British Isles and the Bay of Biscay and likewise from southern Portugal along the Canary Current and the North Equatorial Current to the Caribbean. The resulting rise and fall of sea temperature from 1894—98 to 1920—24, recorded on the map in Fig. 18, coincide by-and-large with the mentioned areas of warm and cold isallobaric advection.

The long term increase of the winds around the anticyclonic gyre shown by Fig. 19 must also increase the component of the drift current normal to the atmospheric isobars, toward the center of the Azores high. As indicated on page 120 that lateral drift current component in the whole belt of westerlies is apt to submerge in the baroclinic zones. South of the Azores high the water displaced towards higher atmospheric pressure does not encounter lighter water and can stay at the surface where, in principle, it can exert a warm advection influence on the surface isotherms. The evidence of the observed sea temperature changes goes, however, definitely in the opposite sense. The cooling by the isobaric component of the drift current, and by the heat loss to the atmosphere, both of which increase with increasing trade-winds, at all times seem to overcomponensate the warming by the lateral component of the drift current. We may thus sum up our findings that both north and south of the Azores high the long term sea temperature change mainly goes in the sense to be expected by the transport of sea isotherms by the isallobaric wind.

The particular question presented by the shift of sign of the correlation coefficient at 50°N in Table 3, is herewith also answered. According to Fig. 19 there must be more than normal loss of heat to the atmosphere, Q_a, and less than normal warm advection, Q_v, by the isobaric component of the drift current north of 50°N, whereas warm advection in both sea and atmosphere is enhanced south of 50°N.

The long trend of weakening of the Iceland low after 1920—24 (see Fig. 5) led to sea temperatures in Iceland waters equaling those in the warm 1890's, and was associated with a widespread warming of the atmosphere in high northern latitudes. The ocean aspect of that climatic change was described by the present author in 1959 and will not be repeated here. Our remaining topic will be to discuss briefly what may be learnt about ocean-atmosphere feedback processes from the synoptic study of the long and short climatic trends earlier in this paper.

C. Feedback from ocean to atmosphere. The oceanic response to both short and long atmospheric trends is to set the thermostat, represented by the sea surface temperature, *lower* in the Labrador—Irminger Sea the deeper is the Iceland cyclone. Simultaneously, the subtropical high intensifies and the ocean sets the thermostat *higher* along the whole western and northern fringe of the anticyclonic current gyre

(1894—98 to 1920—24, Fig. 18), or only slightly higher along its north-western fringe (in short period shifts from low to high index, Fig. 13). Common for both cases is the strengthening of the meridional temperature gradient of the mid-Atlantic between 40° and 50°N. Only in the long trend 1894—98 to 1920—24 does this intensification of oceanic baroclinicity extend all the way from 70° to 20°W longitude, and we will use that case (Figs. 17 and 18) as the best available model of the long term ocean-atmosphere feedback mechanism in the middle latitudes.

An increasing oceanic baroclinicity automatically introduces an increasing atmospheric baroclininicity at the surface and on up through all the layers in convective exchange with the surface. This is facilitated by the fact that the prevailing WSW wind does not deviate much from the orientation of the zone of increasing baroclinicity, and quite often the wind blows right along it.

Increasing baroclinicity in the belt of westerly winds increases the vertical wind shear and the maximum of westerly speed at the tropopause. More upper tropospheric kinetic energy thus becomes available as input into cyclonic storms the further the trend toward increasing baroclinicity proceeds.

The American coast from New England to Newfoundland is known as a place of frequent cyclogenesis on fronts parallel to the coastline, or of intensification of cyclonic disturbances arriving from the west. The reason is again the semi-permanent baroclinicity between the Gulf Stream air and the usually much colder air to its northwest. The trend toward increasing baroclinicity over the stretch from 70°W to 20°W will give a statistically noticeable boost to the cyclogenesis, or other intensification of cyclones, along the coastline and on out into the mid-Atlantic.

Young frontal cyclones always set their course north of the pre-arranged zone of maximum baroclinicity. They will thus usually end their careers as fully developed storm centers near Iceland more often than over the British Isles. The deep storm centers tend to become stagnant, and the Iceland low can be said to be maintained in more or less intense condition by the arrival of the once fast moving but later retarding storm centers from the southwest. Statistically we therefore should get a deeper Iceland low the more efficiently the baroclinic mechanism operates from the Grand Banks to the mid-Atlantic, and this therefore appears to be the reason for the progressive lowering of the Iceland pressure from 1894—98 to 1920—24.

With the progressive intensification of the cyclonic vortex between southern Greenland and Iceland the EKMAN flux makes the surface water diverge from the center, so that colder deepwater reaches to or near the surface. This process can not lower the late winter minimum temperature in the region where each year the thermocline anyway vanishes by winter cooling. But an increased EKMAN divergence can widen the area where that happens, and keep the deepwater longer in contact with the atmosphere, or just thin out any remaining warm surface layer and lower its surface temperature. What all these alternatives amount to is setting the oceanic thermostat lower in the Labrador—Irminger Sea and increasing the baroclinicity along its southern fringe, whereby the chain reaction between ocean and atmosphere continues its course.

At this stage we introduce Fig. 20 as a graphical record of the working of the one-way chain reaction and its eventual reversal. The time scale runs from left to right and covers the period of strengthening of the Iceland low from 1890 to 1920 and its weakening from 1920 to 1940. The sea temperature at the center goes through a maximum a little after 1890, a minimum a little after 1920, and a maximum after 1940 (see curve for 61.5°N in Fig. 5). The two lower curves in Fig. 20 represent the schematic behavior of the heat gain and heat loss of the surface water by the two factors whose fluctuations are believed to be the most important in determining the shifting heat balance. Since we idealize the discussion to be valid at the supposedly stationary cyclonic center, the heat transfer, Q_a, to the atmosphere, which was essential in the heat budget at a location in the strongest part of the cold westerlies, loses its importance. Instead we are concerned with the upwelling as a cooling factor Q_{z_0}, and the Irminger Current, which flows geostrophically northward under the center of the Iceland low, as a warming factor, Q_v. If both cooling and warming operated at normal rate no year to year temperature change would result. The curves in Fig. 20 show the assumed interplay of the deviations from normal of the two factors.

The upwelling responds to changes in intensity of the Iceland low as fast as does the EKMAN drift, which means almost instantaneously. The curve for the cooling rate has therefore been drawn with a positive anomaly (that is, less than normal cooling) when the Iceland low is weak and a negative anomaly (more cooling than normal) at the time of strongest Iceland low.

The Irminger Current, the farthest left branch of the North Atlantic Current, always conveys water of Gulf Stream origin, but it comes presumably from subsurface layers of that current while the topmost, warmest layers have branched off toward points south of the Azores and remain in the anticyclonic gyre. The current finally reaching Iceland waters has also been cooled by lateral mixing at the "cold wall" to its left and, even more importantly, by heat loss to the atmosphere as represented graphically in Fig. 15. Nevertheless, the pulses of heat flux of the Gulf Stream and the North Atlantic Current, in response to a strengthening subtropical high and simultaneously strengthening Iceland low, must be assumed to reach Iceland waters too, although after much attenuation and delay. In Fig. 20 we have therefore arbitrarily placed the maximum heat delivery by the Irminger Current a few years behind the time of maximum atmospheric circulation, and correspondingly the minimum heat delivery a few years after the year of weakest Iceland low.

The equality of cooling rate by upwelling and warming rate by the Irminger Current will then be reached at about half the assumed lag of the extremes of heat delivery behind the extremes in the intensity of the atmospheric circulation. The extremes in sea temperature must coincide with the time of equality of the fluctuating cooling and warming factors, and should occur with a minimum shortly after the year of strongest Iceland low and a maximum shortly after the year of weakest Iceland low.

The presented picture of the heat balance of the ocean at the center of the Iceland low in Fig. 20 is admittedly over-simplified. Its greatest shortcoming probably lies in

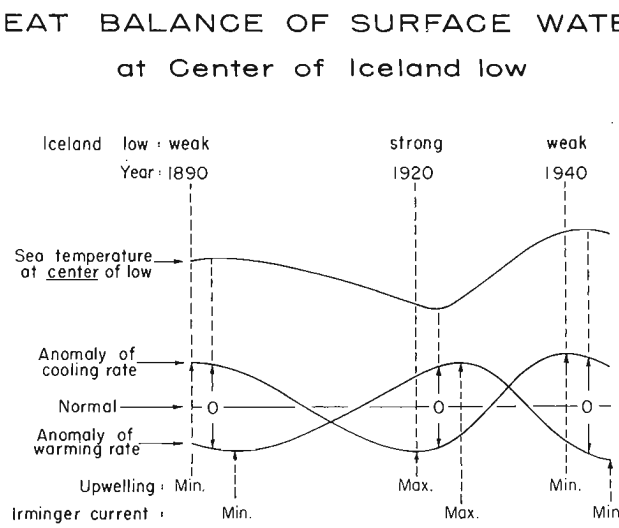

Fig. 20. Suggested model of secular variations in heat balance of the surface water near the center of the Iceland low.

the assumption of a completely stationary Iceland low with a calm central area. In reality, winds of all directions, and quite often strong ones, do occur at such a location. A net heat loss to the atmosphere is bound to result if cold advection and warm advection winds have statistically equal strength and frequency. What matters for our problem is whether such net heat loss is greater when the average Iceland low is deeper, or less deep, than normal. The former case would seem to be more likely and, if so, the heat loss to the atmosphere would go in phase with the heat loss by upwelling in Fig. 20. Proceeding southwards to the belt of maximum westerlies the leat loss to the atmosphere increases, and the role of the upwelling decreases, so that a simplified heat budget like that in Fig. 15 can be assumed to apply.

We can probably claim a little bit of support for the above hypothesis from the correlation tables 1 and 3 in Section A. The sea temperature at 61.5°N (representing the center of the Iceland) correlates with a factor of —0.66 to the depth of that center, and thereby indirectly to its cyclonic vorticity, whereas it correlates poorly, —0.34, with the strength of the westerlies between Iceland and the Azores. On the other hand, the sea temperatures of the test fields centered at 57.5° and 52.5°N correlate well —0.82, with the strength of the westerlies. As mentioned in the discussion of Fig. 5, there is also a little more indication of the sea temperature lagging behind the extremes of the Iceland pressure record in the 61.5°N test field, while no systematic lag of sea temperature behind the extremes of the westerlies is discernable in the adjacent fields to the south.

The ocean-atmosphere feedback in the 2 to 5 year trends must also operate by way of the strengthening and weakening of ocean baroclinicity in the belt 40° to 50°N, which

makes the atmospheric baroclinicity fluctuate in the same phase. The orientation of the ocean isallotherms involved (Fig. 13) is about WNW—ESE while those characterizing the long trend were more truly zonal (Fig. 18). It is therefore natural that the storms activated during the short-period maximum baroclinicity hit Europe as far south as Ireland, and leave a statistical imprint on the average pressure map in the shape of a pronounced trough just west of Ireland. The rear of that type of cyclones brings the cold outbreaks to the Azores, and beyond, and account for the minimum of ocean temperature there in high index years.

The oceanic feedback in the trade-wind belt is perhaps as simple as this:

Maximum trade-wind and maximum westerlies (high index) must occur together, so that the skin friction between atmosphere and earth exerts mutually cancelling torques about the axis of the earth in low and middle latitudes. At that high index stage the fuel consumption of the atmospheric thermodynamic engine in the form of low-latitude heat supply from the earth is likely to be at a maximum. The contribution from the low latitude ocean, which must be the decisive item, is given by the integral over the oceanic trade-wind area A of

$$\int_A Q_a dA = \int_A k W [(e_w - e) + 0.64 (T_w - T_a)] \frac{p}{1000} dA.$$

The trade-wind velocity W is at its maximum at the high index stage, and there is also some evidence that k (assumed constant by SVERDRUP) increases somewhat with wind speed. $(e_w - e)$ and $(T_w - T_a)$ are, according to a set of 59 single measurements from the WYMAN—WOODCOCK (1946) expedition to the Caribbean, negatively correlated with W. The time variations of the Q_a integral (after elimination of the seasonal period) can thus be kept very close to zero. If that were not so, climatic change would take place much faster than actually observed.

J. MALKUS (1960) has issued a timely warning about the "precarious position" of the attempts at treating climatic change quantitatively, by the following numerical example: If an initially balanced energy budget of a tropical ocean were disturbed by an increase of one per cent in the heat of evaporation, a 200 m deep ocean layer would in the course of 50 years cool off by 3°C. No measurements of evaporation integrated over a tropical ocean can pretend to be anywhere near the accuracy of one per cent. Computing, not to speak of predicting, climatic change from field measurements is therefore rather hopeless.

Our main impression of the workings of the important oceanic feedback from the trade-wind zone can therefore only be expressed in terms of a working hypothesis, as follows:

A trend of increasing kinetic energy of the general atmospheric circulation should be indicative of increasing heat energy input from ocean to atmosphere in the trade-wind zone. If so, the increasing energy input would vary parallel to, and would probably be caused by, the increasing strength of the trades. Analogously, a decreasing energy input, and decreasing intensity of the general circulation, would be caused by the

decrease in trade-wind velocity. In that way it can be visualized how the atmospheric circulation, by controlling its own tapping of ocean heat, can lend some degree of persistence to positive or negative changes in its own world-wide energy manifestation.

This purely terrestrial view of climatic change by ocean-atmosphere feedback should, in due course, be supplemented by sifted and tested ideas on solar control of climate.

Concluding Remarks. Whereas the fluctuations in time and space of the atmospheric circulation and the resulting changes in sea surface temperature could be shown to have many clear cut cause-and-effect relationships, quite essential questions still remain unanswered. For instance, although we can probably better understand the persistance of climatic trends, from a couple of years to decades, by studying the interaction of ocean and atmosphere, we have in our data not been able to uncover any clue to the problem of what decides the duration of a trend and its eventual reversal. The shifts of trends do not show the regularity of real periodicities, but yet they do not look like completely random occurrences.

The complexity of the picture must be mainly due to the atmosphere, because atmospheric disturbances travel fast and far and can bring onto the Atlantic scene influences from the whole hemisphere, for instance, represented by the incessantly changing arrangement of the long standing waves in the upper westerlies. A continued study of the ocean-atmosphere interplay (both Pacific and Atlantic) during post-war time, with data from a hemisphere-wide synoptic aerology added (see NAMIAS 1959), would seem to offer possibilities for explaining part of the phenomena which at this stage are shrouded in uncertainty.

Acknowlegements. I wish to acknowledge the generous support from the National Science Foundation for the main bulk of the work here reported on, as well as that of the U.S. Educational Foundation and the John Simon Guggenheim Fund during the early stages of the research. Furthermore, I want to put on record my gratitude to Dr. M. RODEWALD, Seewetteramt, Hamburg, for personally drawing my attention to the research field on climatic change in the oceans, in which his own contributions (in the Deutsche Hydrographische Zeitschrift) have been both numerous and important.

Data for my reserach have been supplied by the Conseil Permanent International pour l'Exploration de la Mer, Copenhagen, and the National Weather Record Center, Asheville, N.C., and the data processing has been in the hands of a team of student helpers at U.C.L.A. For all the helpful services performed I am herewith expressing my sincere thanks.

The present article was brought to its conclusion during my stay at the Scripps Institution of Oceanography, La Jolla, Calif., during the summer of 1961. I acknowledge gratefully the opportunity for discussions with oceanographers of that Institution.

LITERATURE REFERENCES

ÅNGSTRÖM, A. (1920) Application of heat radiation measurements to the problems of the evaporation from lakes and the heat convection at their surfaces. *Geogr. Ann.* h3, Stockholm.

BJERKNES, J. (1959) Temperaturforandringen i Golfstrømmen i tidsrummet for klimaforbedringen i Norden. Vega Lecture 1958, *Ymer* 1959, h2, 148—158.

BULLIG, H. J. (1954) Atlas der Monatswerte von Wassertemperatur, Wind und Bewölkung auf dem Seeweg Europa—Südamerika, *Einzelveröffentlichung* No. 5, Seewetteramt, Hamburg.

DEFANT, A. (1941) Die absolute Topographie des physikalischen Meeresniveaus und der Druckflächen, sowie die Wasserbewegungen im Atlantischen Ozean. *Deutsche Atlantische Expedition «Meteor»* 1925—27, *Wiss. Ergeb.* **6**, 191—260.

DIETRICH, G., and KALLE, K. (1957) *Allgemeine Meereskunde*, Gebrüder Borntraeger, Berlin.

EKMAN, V. W. (1905) On the influence of the earth's rotation on ocean currents. *Arkiv för Matematik, Astronomi och Fysik* **2** (11), 1—52.

FOFONOFF, N. P. (1960—61) Transport computations for the North Pacific Ocean 1955—1960. *Manuscript Report Series* No. 77, Fisheries Research Board of Canada, Pacific Oceanographic Group, Nanaimo, B. C.

HELLAND-HANSEN, B., and NANSEN F. (1917) Temperaturschwankungen des Nordatlantischen Ozeans und in der Atmosphäre. *Videnskapsselskapets Skrifter.* I. Mat.-Naturv. Klasse 1916, No. 9, Kristiania 1917. Contains ample listing of earlier references.

ISELIN, C. O'D. (1936) A study of the circulation of the North Atlantic. *Papers in Physical Oceanography and Meteorology* IV, No. 4, Cambridge, Mass.

LIEPE, H. (1911) Temperaturschwankungen der Meeresoberfläche von Ouessant bis St. Paul-Fels. *Ann. d. Hydr. u. Mar. Met.* **39**, 471—485.

MALKUS, J. (1960) *The air and sea in interaction*, (mimeographed), Woods Hole Oceanographic Institution.

MOSBY, H. (1936). Verdunstung und Strahlung auf dem Meere. *Ann. d. Hydrogr. u. Mar. Meteor*, **64**, 281—286.

MUNK, W. (1950). On the wind-driven ocean circulation. *J. of Meteor.*, **7**, 79—93.

NAMIAS, J. (1959). Recent seasonal interactions between North Pacific waters and the overlying atmospheric circulation. *J. Geophys. Res.*, **64**, 631—646.

NEUMANN, G., and PANDOLFO, J. (1958). *Studies on the interaction between ocean and atmosphere.* Chapter 1, Sea surface temperature anomalies and their relation to the general atmospheric circulation. Contract No. AF 19(604)—1284.

PATTULLO, J. (1957). The seasonal heat budget of the oceans. Ph. D. thesis Univ. of California, Los Angeles.

PETTERSSEN, S., BRADBURY, D., PEDERSEN, K., (1961). Heat exchange and cyclone development on the North Atlantic Ocean. *Scientific Report* No. 4, Contract No. AF 19(604)—7230.

RODEN, G. (1961). On sea surface temperature, cloudiness and wind variations in the tropical Atlantic. In press. *J. of Meteor.*

SMITH, E. H., SOULE, F. M., and MOSBY, O. (1937). The Marion and General Greene expeditions to the Davis Strait and Labrador Sea 1928—31—33—34—35. *U. S. Coast Guard Bull.* No. 19, Part 2, Physical Oceanography, 1—259.

STOMMEL, H. (1957). A survey of ocean current theory. *Deep-Sea Research*, **4**, 149—184.

SVERDRUP, H. U. (1947). Wind-driven currents in a baroclinic ocean; with application to the Equatorial Currents in the eastern Pacific. *Proc. Nat. Acad. Sci.* Washington, D.C., **33**, 318—326.

— JOHNSON, M. W., and FLEMING, R. H. (1942). *The Oceans*, Prentice Hall, Inc., New York.

WYMAN, J., and collaborators (1946). Vertical motion and exchange of heat and water between the air and the sea in the region of the trades. Unpublished report. Woods Hole Oceanographic Institution.

(Manuscript received September 13, 1961)